Elasticity in Ionically Cross-Linked Neurofilament Networks

Norman Y. Yao,[†*] Chase P. Broedersz,[‡] Yi-Chia Lin,[†] Karen E. Kasza,[§] Frederick C. MacKintosh,[‡] and David A. Weitz[†§]

[†]Department of Physics, Harvard University, Cambridge, Massachusetts; [‡]Department of Physics and Astronomy, Vrije Universiteit, Amsterdam, The Netherlands; and [§]School of Engineering and Applied Sciences, Harvard University, Cambridge, Massachusetts

ABSTRACT Neurofilaments are found in abundance in the cytoskeleton of neurons, where they act as an intracellular framework protecting the neuron from external stresses. To elucidate the nature of the mechanical properties that provide this protection, we measure the linear and nonlinear viscoelastic properties of networks of neurofilaments. These networks are soft solids that exhibit dramatic strain stiffening above critical strains of 30–70%. Surprisingly, divalent ions such as Mg^{2+}, Ca^{2+}, and Zn^{2+} act as effective cross-linkers for neurofilament networks, controlling their solidlike elastic response. This behavior is comparable to that of actin-binding proteins in reconstituted filamentous actin. We show that the elasticity of neurofilament networks is entropic in origin and is consistent with a model for cross-linked semiflexible networks, which we use to quantify the cross-linking by divalent ions.

INTRODUCTION

The mechanical and functional properties of cells depend largely on their cytoskeleton, which is comprised of networks of biopolymers that include microtubules, actin, and intermediate filaments. A complex interplay of the mechanics of these networks provides cytoskeletal structure with the relative importance of the individual networks depending strongly on the type of cell (1). The complexity of the intermingled structure and the mechanical behavior of these networks in vivo has led to extensive in vitro studies of networks of individual biopolymers. Many of these studies have focused on reconstituted networks of filamentous actin (F-actin), which dominates the mechanics of the cytoskeleton of many cells (2–7). However, intermediate filaments also form an important network in the cytoskeleton of many cells; moreover, in some cells they form the most important network. For example, in mature axons, neurofilaments, a type IV intermediate filament, are the most abundant cytoskeletal element, overwhelming the amount of actin and outnumbering microtubules by more than an order of magnitude (8). Neurofilaments (NFs) are assembled from three polypeptide subunits, NF-light (NF-L), NF-medium (NF-M), and NF-heavy (NF-H), with molecular masses of 68 kDa, 150 kDa, and 200 kDa, respectively (8). They have a diameter of $d \sim 10$ nm, a persistence length believed to be of order $l_p \sim 0.2$ μm, an in vitro contour length of $L \sim 5$ μm, and an in vivo contour length of $L_I \sim 1.8$ μm (9,10). They share with all other intermediate filaments a conserved sequence that is responsible for the formation of coiled dimers that eventually assemble into tetramers and finally into filaments. Unlike other intermediate filaments, such as vimentin and desmin, NFs have long carboxy terminal extensions that protrude from the filament backbone (11). These highly charged side arms lead to significant interactions among individual filaments, as well as between filaments and ions (12). Networks of NFs are weakly elastic; however, these networks are able to withstand large strains and exhibit pronounced stiffening with increasing strain (13,14). An understanding of the underlying origin of this elastic behavior remains elusive; in particular, even the nature of the cross-linkers, which must be present in such a network, is not known. Such an understanding of the fundamental mechanical properties of these networks of NFs is an essential first step in elucidating the role of NFs in a multitude of diseases (15). However, the elastic behavior of these networks has not as yet been systematically studied.

Here, we report the linear and nonlinear viscoelastic properties of networks of NFs. Although it is well known that the addition of Mg^{2+} is necessary for network gelation, the specific role of Mg^{2+} in relation to network elasticity remains a mystery. In particular, we show that these networks form cross-linked gels analogous to molecularly linked actin networks; the cross-linking is governed by divalent ions such as Mg^{2+} at physiologically relevant millimolar concentrations (16). To explain the origins of the network's elasticity, we apply a semiflexible polymer model that ascribes the network elasticity to the stretching of thermal fluctuations; this quantitatively accounts for the linear and nonlinear elasticity of NF networks, and ultimately even allows us to extract microstructural network parameters such as the persistence length and the average distance between cross-links directly from bulk rheology.

MATERIALS AND METHODS

Materials

NFs were purified from bovine spinal cords using a standard procedure (11,17,18). The fresh tissue was homogenized in the presence of buffer A (0.1 M Mes, 1 mM $MgCl_2$, and 1 mM EGTA, pH 6.8) and then centrifuged

Submitted August 26, 2009, and accepted for publication January 28, 2010.

*Correspondence: nyao@fas.harvard.edu

Editor: Alexander Mogilner.

0006-3495/10/05/2147/7 $2.00

doi: 10.1016/j.bpj.2010.01.062

at a k-factor of 298.8 (Beckman 70 Ti). The crude NF pellet was purified overnight on a discontinuous sucrose gradient with 0.8 M sucrose (5.9 ml), 1.5 M sucrose (1.3 ml), and 2.0 M sucrose (1.0 ml). After overnight sedimentation, the concentration of the purified NF was determined with a Bradford Assay using bovine serum albumin as a standard. The purified NF was dialyzed against buffer A containing 0.8 M sucrose for 76 h, and 120-μl aliquots were then flash-frozen in liquid nitrogen and stored at -80°C.

Bulk rheology

The mechanical response of the cross-linked NF networks was measured with a stress-controlled rheometer (HR Nano, Malvern Instruments, Worcestershire, UK) using a 20-mm-diameter 2° stainless steel cone plate geometry and a gap size of 50 μm. Before rheological testing, the NF samples were thawed on ice, after which they were quickly pipetted onto the stainless steel bottom plate of the rheometer in the presence of varying concentrations of Mg^{2+}. We utilized a solvent trap to prevent our networks from drying. To measure the linear viscoelastic moduli, we utilized a large-amplitude oscillatory shear measurement (LAOS); we applied an oscillatory stress of the form $\sigma(t) = A\sin(\omega t)$, where A is the amplitude of the stress and ω is the frequency. The resulting strain was of the form $\gamma(t) = B\sin(\omega t + \delta)$ and yields the storage modulus $G'(\omega) = A/B\cos(\delta)$ and the loss modulus $G''(\omega) = A/B\sin(\delta)$. To determine the frequency dependence of the linear moduli, $G'(\omega)$,$G''(\omega)$ were sampled over a range of frequencies from 0.006 to 25 rad/s. In addition, we probed the stress dependence of the network response by measuring $G'(\omega)$,$G''(\omega)$ at a single frequency, varying the amplitude of the oscillatory stress. To probe nonlinear behavior, we utilized a differential measurement, an effective probe of the tangent elastic modulus, which for a viscoelastic solid such as NFs provides consistent nonlinear measurements of elasticity in comparison to other nonlinear methods (19–21). A small oscillatory stress was superimposed on a steady prestress, σ, resulting in a total stress of the form $\sigma(t) = \sigma + |\delta\sigma|\sin(\omega t)$. The resultant strain was $\gamma(t) = \gamma + |\delta\gamma|\sin(\omega t + \phi)$, yielding a differential elastic modulus $K'(\sigma) = \delta\sigma/\delta\gamma\cos(\phi)$ and a differential viscous modulus $K''(\sigma) = \delta\sigma/\delta\gamma\sin(\phi)$ (2).

Scaling parameters

To compare the experiments with theory, we collapsed the differential measurements into a single master curve by scaling the stiffness, K', and stress, σ, by two free parameters for each data set. According to theory, the stiffness versus stress should have a single universal form apart from these two scale factors. We determined the scale factors by cubic-spline fitting the data sets to piecewise polynomials; these polynomials were then scaled onto the predicted stiffening curve using a least-squares regression.

RESULTS AND DISCUSSION

To quantify the mechanical properties of NFs, we probed the linear viscoelastic moduli of the network during gelation, which takes approximately 1 h; we characterized this by continuously measuring the linear viscoelastic moduli at a single frequency, $\omega = 0.6$ rad/s. Gelation of these networks was initiated by the addition of millimolar amounts of Mg^{2+}, and during this process we found that the linear viscoelastic moduli increased rapidly before reaching a plateau value. We measured the frequency dependence of the linear viscoelastic moduli over a range of NF and Mg^{2+} concentrations. To ensure that we were probing the linear response, we maintained a maximum applied stress amplitude of < 0.01 Pa, corresponding to strains $< 5\%$. We found that the linear moduli are frequency-independent for all tested frequencies, 0.006–25 rad/s. In addition, NF networks behave as a viscoelastic solid for all ranges of Mg^{2+} concentrations tested and the linear storage modulus is always at least an order of magnitude greater than the linear loss modulus (Fig. 1). This is indicative of a cross-linked gel and allows us to define a plateau elastic modulus, G_0 (22).

The elasticity of NF networks is highly nonlinear; above critical strains, γ_c, of 30–70%, the networks show stiffening up to LAOS strains of 300% (23) (Fig. 2). A shear strain of 300% corresponds to at most a 150% extensional strain on the filament level. LAOS deforms a material through a range of stress states throughout both the linear and nonlinear regime, and deconvoluting this information to determine an effective strain is thus difficult. It is also important to note that stress-controlled LAOS measures only the first harmonic strain response and ignores higher harmonic contributions to the strain. For highly nonlinear materials, such as NF networks, the LAOS strain is thus unreliable. The measurements in Fig. 2 qualitatively demonstrate the nonlinearity of the networks, which occurs for a wide variety of Mg^{2+} and NF concentrations. In addition, by varying the MF concentration, c_{NF}, and the Mg^{2+} concentration, c_{Mg}, we can finely tune the linear storage modulus, G_0, over a wide range of values (Fig. 3). The strong dependence of G_0 on Mg^{2+} concentration is reminiscent of actin networks cross-linked with incompliant cross-linkers such as scruin and heavy meromyosin (2,24–26), which suggests that in the case of NFs, Mg^{2+} effectively acts as a cross-linker, leading to the formation of a viscoelastic network. Within this model, the NFs are cross-linked ionically on length scales comparable to their persistence length; hence, they should behave as a cross-linked semiflexible biopolymer network. We therefore hypothesize that the network elasticity is purely due to the stretching out of transverse thermal fluctuations of the filaments, which are assumed to be inextensible. These thermally driven fluctuations reduce NF extension, resulting in an entropic spring. To consider these entropic effects, we

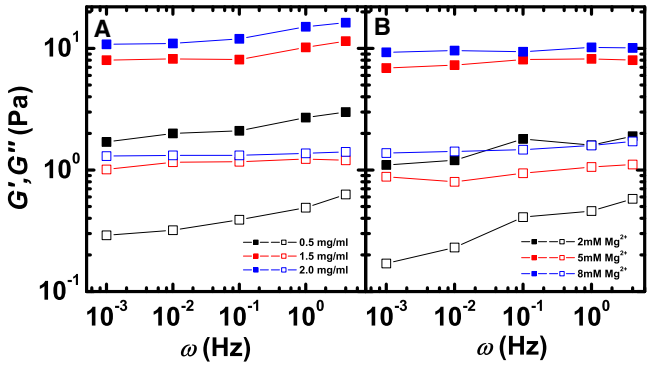

FIGURE 1 The frequency dependence of the linear viscoelastic moduli of cross-linked networks for a variety of NF and Mg^{2+} concentrations. (*A*) Variations of the moduli at constant Mg^{2+} concentration (5 mM) and changing filament concentration. (*B*) Variations of the moduli at constant NF concentration (1.5 mg/ml) and changing Mg^{2+} concentration.

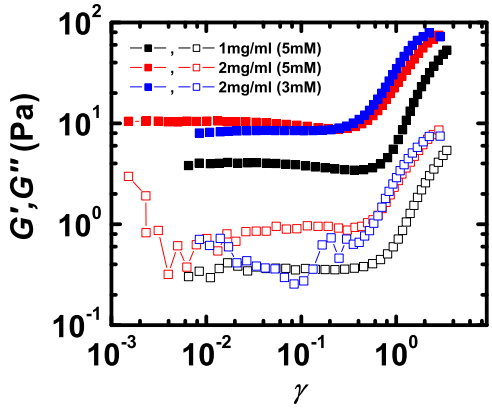

FIGURE 2 The strain-stiffening behavior of NF networks at various Mg^{2+} and NF concentrations. G' is the elastic modulus (*solid squares*) and G'' the viscous modulus (*open squares*). Dramatic nonlinearities are seen at critical strains ranging from 30% to 70%.

can model the network as an isotropic collection of thermally fluctuating semiflexible polymer segments of length l_c, where l_c is the average distance between ionic cross-link nodes. A convincing test of the hypothesis of entropic elasticity, as well as of the role of divalent ions as cross-linkers between NFs, is the nonlinear behavior of the network. When the thermal fluctuations are pulled out by increasing strain, the elastic modulus of the network exhibits a pronounced increase.

To probe this nonlinear elasticity of NF networks, we measured the differential or tangent elastic modulus $K'(\sigma)$ at a constant frequency, $\omega = 0.6$ rad/s for a variety of NF and Mg^{2+} concentrations. If the network elasticity is indeed entropic in origin, this can provide a natural explanation for the nonlinear behavior in terms of the nonlinear elastic force-extension response of individual filaments that deform uniformly according to the macroscopic strain field. Here, the force required to extend a single filament diverges as the length approaches the full extension, l_c, according to $F_N \sim l/(l\text{-}l_c)^2$ (27–29). Provided the network deformation is affine, its macroscopic shear stress is primarily due to the stretching and compression of the individual elements of the network. The expected divergence of the single-filament tension leads to a scaling of dF/dl ~ $F_N^{3/2}$; we therefore expect a scaling of network stiffness with stress of the form $K'(\sigma) \sim \sigma^{3/2}$ in the highly nonlinear regime (2). Indeed, NF networks formed in the presence of divalent ions show remarkable consistency with this affine thermal model for a wide range of NF and Mg^{2+} concentrations (Fig. 4). This consistency provides evidence of the entropic nature of the network's nonlinear elasticity (2,28).

The affine thermal model also suggests that the functional form of the data should be identical for all values of c_{NF} and the concentration of the proposed ionic cross-links, c_{Mg}. To test this, we scaled all the data sets for $K'(\sigma)$ onto a single master curve. This is accomplished by scaling the modulus by a factor $\tilde{G}$ and the stress by a factor $\tilde{\sigma}$. Consistent with the theoretical prediction, all the data from various NF and Mg^{2+} concentrations can indeed be scaled onto a universal curve (Fig. 5). The scale factor for the modulus is the linear shear modulus $\tilde{G} = G_0$, whereas the scale factor for the stress is a measure of the critical stress, σ_c, at which the network begins to stiffen. This collapse provides additional evidence that the nonlinear elasticity of cross-linked NF networks is due to the entropy associated with single filament stretching.

To explore the generality of the ionic cross-linking behavior, we used other divalent ions, including Ca^{2+} and Zn^{2+}. We found that the effects of both of these ions on the nonlinear rheological behavior are nearly identical to those of Mg^{2+}; they also cross-link NF networks into weak elastic gels. This lack of dependence on the specific

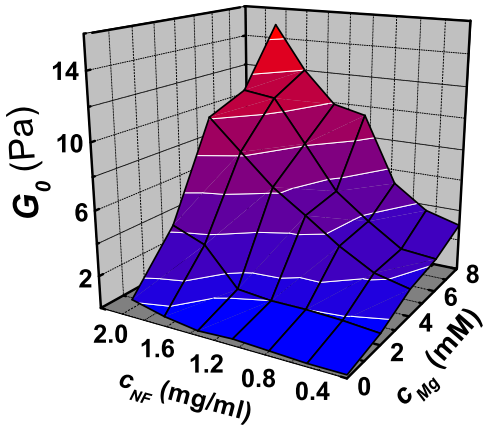

FIGURE 3 The linear elastic modulus, G_0, as a function of c_{NF} and c_{Mg}. The network elasticity can be finely tuned over an order of magnitude by varying the concentration of the cross-linker Mg^{2+} and the NF concentration. The essential role of Mg^{2+} as a network cross-linker is evinced by the markedly stronger dependence on c_{NF} for increasing divalent ion concentration.

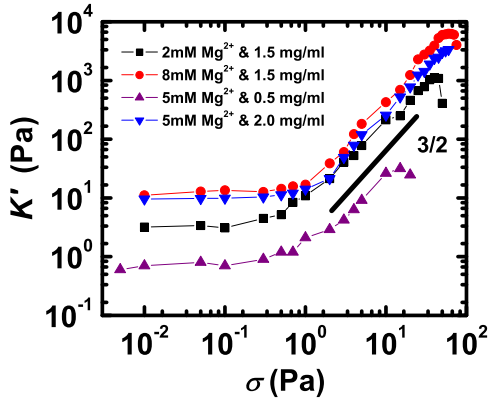

FIGURE 4 The dependence of $K'(\sigma)$ on σ for a variety of NF and Mg^{2+} concentrations. The effects of varying c_{Mg} at a constant filament concentration of 1.5 mg/ml and c_{NF} at a constant divalent ion concentration of 5 mM are shown. As expected, the linear elastic modulus and the breakage stress differ; however, all data show an exponent of ~3/2 (*black line*), in agreement with the affine thermal model.

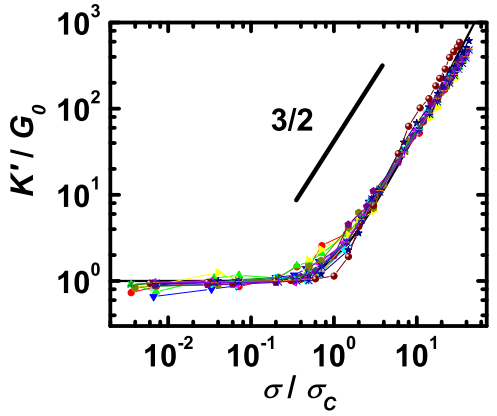

FIGURE 5 Collapse of all data sets of the σ dependence of K' onto a single universal curve. The scaling parameters are G_0, the linear elastic modulus, and σ_c, the critical stress. These parameters are calculated using a least-squares regression. Data shown represent varying filament concentrations from 0.5 to 2.2 mg/ml and varying divalent ion concentrations from 2 to 8 mM. The data points at the high-stress end that show a downturn just before network failure are likely due to network breakage and are therefore removed to avoid improper influence on regression parameters.

ionic cross-link lends evidence that the interaction between filaments and ions is electrostatic in nature.

The ability to scale all data sets of $K'(\sigma)$ onto a single universal curve also provides a means to convincingly confirm that the linear elasticity is entropic in origin. Furthermore, with a scaling analysis we can demonstrate that the typical distance between cross-links in the network is determined by the concentration of divalent ions. To accomplish this, we derived an expression from a microscopic model that relates the two scaling parameters G_0 and σ_c to each other. The force required for a small extension, δl, of a thermally fluctuating semiflexible polymer segment of length l_c can be derived from the wormlike chain model, giving $F_0 \sim (\kappa^2/k_BT)\delta l/l_c^4$. Assuming an affine deformation, and accounting for an isotropic distribution of filaments, the full expression for the linear elastic modulus of the network is given by

$$G_0 = 6\rho k_B T \frac{\ell_p^2}{\ell_c^3}, \quad (1)$$

where $\kappa = k_BTl_p$ is the bending rigidity of NFs, k_BT is the thermal energy, and ρ is the filament-length density (2,28,30–32). The density ρ is also proportional to the mass density c_{NF}, and is related to the mesh size, ξ, of the network by $\xi \sim 1/\sqrt{\rho}$ (33). Although the inverse root dependence is general, the precise prefactor depends on the geometry of the network; for instance, for an ordered cubic network, the precise expression is $\xi = \sqrt{3/\rho}$. Furthermore, the model predicts a characteristic filament tension proportional to κ/l_c^2, and a corresponding characteristic stress (2,24,28)

$$\sigma_c = \rho k_B T \frac{\ell_p}{\ell_c^2}. \quad (2)$$

In principle, divalent ions could be playing a much more complicated role than simply cross-linking the network; for example, if the ions were also affecting single-filament parameters such as the persistence length, then the direct analogy to molecular linkers would not provide a complete picture.

Combining Eqs. 1 and 2 allows us to scale out the cross-linking distance, leaving only a dependence on temperature and the filament persistence length. In this case, we would expect the scaling $c_{NF}^{1/2}G_0 \sim \sigma_c^{3/2}$, where the prefactor should depend only on k_BT and l_p; although the prefactor will differ for different types of filaments, it should be the same for different networks composed of the same filament type and at the same temperature, such as in our case. Thus, plotting $c_{NF}^{1/2}G_0$ as a function of σ_c for different NF networks at the same temperature should result in collapse of the data onto a single curve characterized by a 3/2 power law. This even includes systems with different divalent ions or different ionic concentrations. For a variety of divalent ions and different ionic concentrations, we find that $c_{NF}^{1/2}G_0 \sim \sigma_c^z$, where $z = 1.54 \pm 0.14$, in excellent agreement with this model (Fig. 6). It is essential to note that the 3/2 exponent found here is not a direct consequence of the 3/2 exponent obtained in Fig. 5, which characterizes the highly nonlinear regime. Instead, the plot of $c_{NF}^{1/2}G_0$ as a function of σ_c probes the underlying mechanism and extent of the linear elastic regime. Although the slope of 3/2 captures the entropic stretching, the intercept of the y axis is set by the persistence length. Thus, the collapse of the data onto a single master curve for various ionic species and concentrations indicates that varying divalent ion concentration does not have a significant effect on l_p. This implies that the strong dependence of the linear and nonlinear rheological properties of NF networks on c_{Mg} is largely due to the dependence of l_c

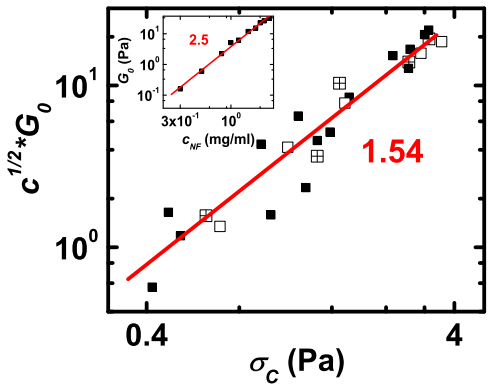

FIGURE 6 The dependence of $c_{NF}^{1/2}G_0$ on σ_c. The solid line is the result of a regression fit to the data and depicts an exponent of 1.54. This is in agreement with the affine thermal model, which predicts an exponent of 3/2. Data were obtained for Mg^{2+} (*solid squares*), Ca^{2+} (*open squares*), and Zn^{2+} (*crossed squares*). (*Inset*) Dependence of G_0 on c_{NF}. An exponent of 2.5 was obtained from regression. This is also consistent with the affine thermal model, which predicts an exponent of 2.2.

on c_{Mg}, supporting the claim that divalent ions are acting as effective cross-linkers between NFs.

We expect cross-linking to occur on the scale of the entanglement length, $l_e \sim l_p^{1/5}/\rho^{2/5}$, which sets the typical distance for binary collisions between thermally fluctuating semiflexible polymer chains. For a fixed-ratio mole ratio, R, of Mg^{2+} to NFs, $l_c \sim {c_{NF}}^{-2/5}$ (28,30,34,35). Thus, inserting this concentration dependence into Eq. 1, we expect the linear storage modulus to scale with NF concentration as $G_0 \sim {c_{NF}}^{11/5}$ (28,30). For $R = 1000$, we find an approximate scaling of $G_0 \sim {c_{NF}}^{2.5}$, consistent with the predicted power law (Fig. 6). It is interesting that the stronger concentration dependence of G_0 may be a consequence of the dense cross-linking we observe. Specifically, for densely cross-linked networks corresponding to a minimum l_c on the order of the typical spacing between filaments, ξ, as we observe here, the model in Eq. 1 predicts $G_0 \sim {c_{NF}}^{2.5}$ (28). The agreement with the affine thermal model in both the linear and nonlinear regimes confirms the existence of an ionically cross-linked NF gel whose elasticity is due to the pulling out of thermal fluctuations.

The ability of the affine thermal model to explain the elasticity of the NF network also suggests that we should be able to quantitatively extract network parameters from the bulk rheology. The model predicts that

$$l_p = \frac{1}{36}\rho\frac{k_B T G_0^2}{\sigma_c^3} \tag{3}$$

and

$$l_c = \frac{1}{6}\rho\frac{k_B T G_0}{\sigma_c^2}, \tag{4}$$

where $\rho \approx 2.1 \times 10^{13}\ m^{-2}$ for NF networks at a concentration of 1 mg/mL. This yields a persistence length $l_p \approx 0.2\ \mu m$, which is in excellent agreement with previous single-filament measurements (10). In addition, we find that $l_c \approx 0.3\ \mu m$, which is close to the theoretical mesh size $\xi \approx 1/\sqrt{\rho} \approx 0.26\ \mu m$. Surprisingly, this is far below the mesh size of 4 μm inferred from tracer particle motion (1). Such particle tracking only provides an indirect measure: in weakly cross-linked networks, for instance, even particles that are larger than the average interfilament spacing will tend to diffuse slowly. At a given concentration, particles substantially larger than the average mesh size can move through a meshwork that is highly inhomogeneous with large voids. Within the limits of the resolution of confocal images, we were able to rule out significant network bundling and a large inhomogeneous mesh size. These limits prevent us from directly extracting a value for the mesh size, but allow us to estimate an upper bound on the mesh size of ~1 μm. This would, for instance, rule out significant bundling of the network.

To further elucidate the cross-linking behavior of Mg^{2+}, we explored the dependence of l_c on both c_{Mg} and c_{NF}. Within the affine thermal model, we expect the cross-linking distance to be governed by the concentration of a specific molecular cross-linker, which sets the average distance between cross-link nodes. The exact form of the dependence of l_c on the concentration of cross-links depends on the details of the biochemical interaction, the effectiveness of the cross-linking, and the level of cross-link saturation. For a variety of molecular cross-linking proteins, the dependence of l_c on cross-linker concentration is well described by a power law. However, the exponent of this power law depends on the properties of the specific cross-linker: Thus, assuming that Mg^{2+} is acting as a cross-linker, the filling fraction of potential binding sites for effective cross-linking between two filaments scales as R^X. Since topological entanglements between neighboring filaments set the lengthscale for cross-linking, we would expect that $l_c \sim l_e/R^X$, implying that for fixed c_{NF}, $l_c \sim {c_{Mg}}^{-X}$, whereas for fixed R, $l_c \sim {c_{NF}}^{-2/5}$. Naively, we would expect that $X \approx 1$, which implies that doubling the concentration of Mg^{2+} would halve the average distance between cross-links. Empirically, we find a much weaker dependence on c_{Mg}, where $l_c \sim {c_{Mg}}^{-0.2}$ at constant c_{NF} (Fig. 7). A similarly weak dependence was seen previously with actin networks in the presence of heavy meromysin where X was found to be 0.4 (26). We note that there is an excess of Mg^{2+} ions available for cross-linking, since the number density of cross-links/m^3 is $N_C = \rho/l_c \approx 7.5 \times 10^{19}\ m^{-3}$, whereas the number density of ions in a standard 5-mM Mg^{2+} concentration is $N \approx 30 \times 10^{23}$. Although it is likely that multiple ions mediate a single cross-link, these numbers suggest that only a small fraction of the ions are involved in forming effective network cross-links. This saturation of ionic cross-links may be responsible for the observed weak power law in the concentration dependence of l_c on c_{Mg}. In addition, we found that at a constant molar ratio, $l_c \sim {c_{NF}}^{-0.5}$, consistent with the predicted $-2/5$ exponent (Fig. 7, *inset*). The direct dependence of the cross-linking distance l_c on c_{Mg} further confirms

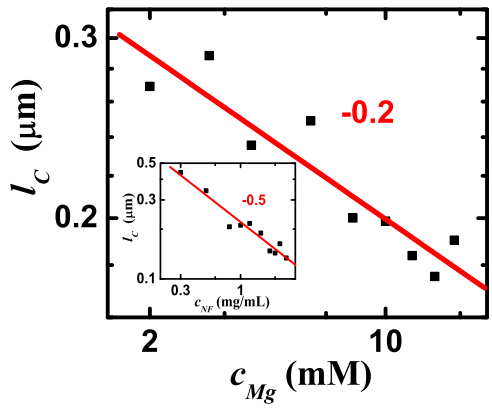

FIGURE 7 Dependence of l_c on c_{NF} at a fixed molar ratio of 1000. The solid line is the result of a regression fit and exhibits an exponent of -0.5. This is consistent with the affine thermal model, which predicts an exponent of $-2/5$. (*Inset*) Dependence of l_c on c_{Mg} at a fixed filament concentration, with an exponent of -0.2 obtained by a regression fit.

the role of Mg^{2+} as the effective ionic cross-linker of the NF networks. We propose that divalent ions mediate an effective cross-linking interaction similar to traditional molecular cross-linking proteins. The generality of this cross-linking behavior for various divalent ion species suggests that this interaction may be purely electrostatic in nature. NF side arms are negatively charged, flexible, thermally collapsed chains, and we envision that the divalent ions are interwoven into the entangled side-arm structure. Although side arms of one chain will likely cross-link within themselves, only cross-links between two different chains will contribute to network elasticity. This cross-linking will likely involve many side arms of one filament interacting with the backbone and side arms of another filament. Remarkably, increasing the concentration of the proposed ionic cross-linker enhances the network toughness by increasing the breakage stress by almost an order of magnitude (Fig. 4). Our findings demonstrate both the entropic origin of NF network elasticity and the role of Mg^{2+} as an effective ionic cross-linker.

CONCLUSIONS

We measured the linear and nonlinear viscoelastic properties of cross-linked NF solutions over a wide range Mg^{2+} and NF concentrations. NFs are interesting intermediate filament networks whose nonlinear elasticity has not been studied systematically. We show that the NF networks form densely cross-linked gels, whose elasticity can be well understood within an affine entropic framework. We provide direct quantitative calculations of l_p and l_c from bulk rheology using this model. Furthermore, our data provides evidence that Mg^{2+} acts as the effective ionic cross-linker in the NF networks. The weaker-than-expected dependence we observe suggests that Mg^{2+} may be near saturation in our networks. Future experimental work with other multivalent ions is required to better understand the electrostatic interaction between filaments and cross-links; this would lead to a better microscopic understanding of the effects of electrostatic interactions in the cross-linking of NF networks. Moreover, the effect of divalent ions on the cross-linking of networks of other intermediate filaments would be very interesting to explore.

The authors acknowledge insights of and discussions with Sirfyl Pincus.

This work was supported in part by the National Science Foundation (DMR-0602684 and CTS-0505929), the Harvard Materials Research Science and Engineering Center (DMR-0213805), the United States Department of Energy (FG02-97ER25308), and the Stichting voor Fundamenteel Onderzoek der Materie (FOM/NWO). C.P.B. acknowledges the hospitality of Harvard University.

REFERENCES

1. Rammensee, S., P. A. Janmey, and A. R. Bausch. 2007. Mechanical and structural properties of in vitro neurofilament hydrogels. *Eur. Biophys. J.* 36:661–668.
2. Gardel, M. L., J. H. Shin, …, D. A. Weitz. 2004. Elastic behavior of cross-linked and bundled actin networks. *Science.* 304:1301–1305.
3. Hinner, B., M. Tempel, …, E. Frey. 1998. Entanglement, elasticity, and viscous relaxation of actin solutions. *Phys. Rev. Lett.* 81:2614–2617.
4. Tharmann, R., M. M. Claessens, and A. R. Bausch. 2006. Micro- and macrorheological properties of actin networks effectively cross-linked by depletion forces. *Biophys. J.* 90:2622–2627.
5. Storm, C., J. J. Pastore, …, P. A. Janmey. 2005. Nonlinear elasticity in biological gels. *Nature.* 435:191–194.
6. Xu, J. Y., W. H. Schwarz, …, T. D. Pollard. 1998. Mechanical properties of actin filament networks depend on preparation, polymerization conditions, and storage of actin monomers. *Biophys. J.* 74: 2731–2740.
7. Käs, J., H. Strey, …, P. A. Janmey. 1996. F-actin, a model polymer for semiflexible chains in dilute, semidilute, and liquid crystalline solutions. *Biophys. J.* 70:609–625.
8. Wong, P. C., J. Marszalek, …, D. W. Cleveland. 1995. Increasing neurofilament subunit NF-M expression reduces axonal NF-H, inhibits radial growth, and results in neurofilamentous accumulation in motor neurons. *J. Cell Biol.* 130:1413–1422.
9. Wagner, O. I., J. Ascaño, …, E. L. Holzbaur. 2004. The interaction of neurofilaments with the microtubule motor cytoplasmic dynein. *Mol. Biol. Cell.* 15:5092–5100.
10. Dogic, Z., J. Zhang, …, A. G. Yodh. 2004. Elongation and fluctuations of semiflexible polymers in a nematic solvent. *Phys. Rev. Lett.* 92:125503.
11. Leterrier, J. F., J. Käs, …, P. A. Janmey. 1996. Mechanical effects of neurofilament cross-bridges. Modulation by phosphorylation, lipids, and interactions with F-actin. *J. Biol. Chem.* 271:15687–15694.
12. Kumar, S., and J. H. Hoh. 2004. Modulation of repulsive forces between neurofilaments by sidearm phosphorylation. *Biochem. Biophys. Res. Commun.* 324:489–496.
13. Wagner, O. I., S. Rammensee, …, P. A. Janmey. 2007. Softness, strength and self-repair in intermediate filament networks. *Exp. Cell Res.* 313:2228–2235.
14. Kreplak, L., H. Bär, …, U. Aebi. 2005. Exploring the mechanical behavior of single intermediate filaments. *J. Mol. Biol.* 354:569–577.
15. Kumar, S., X. H. Yin, …, M. E. Paulaitis. 2002. Relating interactions between neurofilaments to the structure of axonal neurofilament distributions through polymer brush models. *Biophys. J.* 82:2360–2372.
16. Black, S., H. Yu, …, R. L. Medcalf. 2001. Physiologic concentrations of magnesium and placental apoptosis: prevention by antioxidants. *Obstet. Gynecol.* 98:319–324.
17. Delacourte, A., G. Filliatreau, …, J. Schrevel. 1980. Study of the 10-nm-filament fraction isolated during the standard microtubule preparation. *Biochem. J.* 191:543–546.
18. Leterrier, J. F., and J. Eyer. 1987. Properties of highly viscous gels formed by neurofilaments in vitro. A possible consequence of a specific inter-filament cross-bridging. *Biochem. J.* 245:93–101.
19. Yao, N. Y., R. Larsen, and D. A. Weitz. 2008. Probing nonlinear rheology with inertio-elastic oscillations. *J. Rheol.* 52:1013–1025.
20. Baravian, C., G. Benbelkacem, and F. Caton. 2007. Unsteady rheometry: can we characterize weak gels with a controlled stress rheometer? *Rheol. Acta.* 46:577–581.
21. Baravian, C., and D. Quemada. 1998. Using instrumental inertia in controlled stress rheometry. *Rheol. Acta.* 37:223–233.
22. Rubenstein, M., and R. Colby. 2004. Polymer Physics. Oxford University Press, Oxford, United Kingdom.
23. Weitz, D. A., and P. A. Janmey. 2008. The soft framework of the cellular machine. *Proc. Natl. Acad. Sci. USA.* 105:1105–1106.
24. Gardel, M. L., J. H. Shin, …, D. A. Weitz. 2004. Scaling of F-actin network rheology to probe single filament elasticity and dynamics. *Phys. Rev. Lett.* 93:188102.
25. Bausch, A. R., and K. Kroy. 2006. A bottom-up approach to cell mechanics. *Nat. Phys.* 2:231–238.

26. Tharmann, R., M. Claessens, and A. R. Bausch. 2007. Viscoelasticity of isotropically cross-linked actin networks. *Phys. Rev. Lett.* 98:088103.

27. Bustamante, C., J. F. Marko, …, S. Smith. 1994. Entropic elasticity of λ-phage DNA. *Science.* 265:1599–1600.

28. MacKintosh, F. C., J. Käs, and P. A. Janmey. 1995. Elasticity of semiflexible biopolymer networks. *Phys. Rev. Lett.* 75:4425–4428.

29. Fixman, M., and J. Kovac. 1973. Polymer conformational statistics 3. Modified Gaussian models of stiff chains. *J. Chem. Phys.* 58: 1564–1568.

30. Semenov, A. N. 1986. Dynamics of concentrated solutions of rigid-chain polymers. 1. Brownian-motion of persistent macromolecules in isotropic solution. *J. Chem. Soc., Faraday Trans. II.* 82: 317–329.

31. Gittes, F., and F. C. MacKintosh. 1998. Dynamic shear modulus of a semiflexible polymer network. *Phys. Rev. E.* 58:R1241–R1244.

32. Broedersz, C. P., C. Storm, and F. C. MacKintosh. 2009. Effective-medium approach for stiff polymer networks with flexible cross-links. *Phys. Rev. E Stat. Nonlin. Soft Matter Phys.* 79:11.

33. Schmidt, C. F., M. Barmann, …, E. Sackmann. 1989. Chain dynamics, mesh size, and diffusive transport in networks of polymerized actin: a quasielastic light-scattering and microfluorescence study. *Macromolecules.* 22:3638–3649.

34. Odijk, T. 1983. On the statistics and dynamics of confined or entangled stiff polymers. *Macromolecules.* 16:1340–1344.

35. Odijk, T. 1995. Stiff chains and filaments under tension. *Macromolecules.* 28:7016–7018.